

An acetyltransferase-independent function of Eso1 regulates centromere cohesion

Su-Jiun Lin^a, Claudia Tapia-Alveal^a, Omar J. Jabado^b, Doris Germain^c, and Matthew J. O'Connell^{a,d,*}

^aDepartment of Oncological Sciences, ^bDepartment of Genetics and Genomic Sciences, ^cDepartment of Hematology and Oncology, and ^dGraduate School of Biomedical Sciences, Icahn School of Medicine at Mount Sinai, New York, NY 10029

ABSTRACT Eukaryotes contain three essential Structural Maintenance of Chromosomes (SMC) complexes: cohesin, condensin, and Smc5/6. Cohesin forms a ring-shaped structure that embraces sister chromatids to promote their cohesion. The cohesiveness of cohesin is promoted by acetylation of N-terminal lysines of the Smc3 subunit by the acetyltransferases Eco1 in *Saccharomyces cerevisiae* and the homologue, Eso1, in *Schizosaccharomyces pombe*. In both yeasts, these acetyltransferases are essential for cell viability. However, whereas non-acetylatable Smc3 mutants are lethal in *S. cerevisiae*, they are not in *S. pombe*. We show that the lethality of a temperature-sensitive allele of *eso1* (*eso1-H17*) is due to activation of the spindle assembly checkpoint (SAC) and is associated with premature centromere separation. The lack of cohesion at the centromeres does not correlate with Psm3 acetylation or cohesin levels at the centromeres, but is associated with significantly reduced recruitment of the cohesin regulator Pds5. The SAC activation in this context is dependent on Smc5/6 function, which is required to remove cohesin from chromosome arms but not centromeres. The mitotic defects caused by Smc5/6 and Eso1 dysfunction are cosuppressed in double mutants. This identifies a novel function (or functions) for Eso1 and Smc5/6 at centromeres and extends the functional relationships between these SMC complexes.

Monitoring Editor

Mark J. Solomon
Yale University

Received: Aug 16, 2016

Revised: Oct 11, 2016

Accepted: Oct 12, 2016

INTRODUCTION

During the course of the cell cycle, chromosomes undergo massive reengineering to allow gene expression, DNA repair, DNA replication, and finally their compaction and segregation at mitosis. Multi-protein Structural Maintenance of Chromosomes (SMC) complexes, together with DNA topoisomerases, modulate the dynamics of chromosomes as they confront these challenges.

Each SMC complex contains a heterodimer of Smc proteins. These are large coiled-coil proteins with N-terminal Walker A and C-terminal Walker B ATP-binding motifs (Harvey *et al.*, 2002).

This article was published online ahead of print in MBoC in Press (<http://www.molbiolcell.org/cgi/doi/10.1091/mbc.E16-08-0596>) on October 19, 2016.

The authors declare no competing financial interests.

*Address correspondence to: Matthew J. O'Connell (matthew.oconnell@mssm.edu).

Abbreviations used: GFP, green fluorescent protein; HU, hydroxyurea; MMS, methyl methanesulfonate; OTR, centromeric outer repeats; SAC, spindle assembly checkpoint; SMC, structural maintenance of chromosomes.

© 2016 Lin *et al.* This article is distributed by The American Society for Cell Biology under license from the author(s). Two months after publication it is available to the public under an Attribution-Noncommercial-Share Alike 3.0 Unported Creative Commons License (<http://creativecommons.org/licenses/by-nc-sa/3.0>).

"ASCB®," "The American Society for Cell Biology®," and "Molecular Biology of the Cell®" are registered trademarks of The American Society for Cell Biology.

Eukaryotic SMC complexes are made up of condensin (Smc2 and 4), cohesin (Smc1 and 3), and Smc5/6 (Smc5 and 6). The Smc proteins contain two coiled-coil domains separated by a flexible hinge, where the proteins fold back on themselves to enable N- and C-terminal interactions through ATP binding by the Walker A and B motifs. These folded proteins interact at the hinge domains to form a V-shaped heterodimer. The globular domains are joined by a kleisin subunit to form a ring-shaped structure. Each complex contains a number of unique non-Smc subunits that form an additional layer of specificity for the function(s) of each complex (Hirano, 2006).

Condensin, together with type II DNA topoisomerases, controls the decatenation and condensation of chromosomes that is essential for sister chromatid separation (Hirano, 2005). Cohesin embraces replicated chromatids and, in doing so, facilitates DNA repair by homologous recombination and ensures sister chromatids are equally segregated into daughter cells at anaphase. Cohesin also controls gene expression by locus insulation and modulates the progression of replication forks (Parelho *et al.*, 2008; Rubio *et al.*, 2008; Wendt *et al.*, 2008; Nasmyth and Haering, 2009; Terret *et al.*, 2009; Merckenschlager and Odom, 2013). The function(s) of the third complex, Smc5/6, have remained enigmatic, but most studies have focused on recombinational repair of double-stranded DNA breaks

and collapsed replication forks (Murray and Carr, 2008). However, the core Smc5/6 genes are essential for viability, with null mutants initiating but unable to complete chromosome segregation (Verkade et al., 1999; Harvey et al., 2004; Tapia-Alveal et al., 2014a).

During interphase, cohesin is highly dynamic and becomes enriched at sites of DNA damage (Sjogren and Nasmyth, 2001). As most eukaryotic cells enter prophase, the majority of cohesin is stripped off chromosome arms by a poorly characterized mechanism, and cohesin complexes remain physically intact (Tomonaga et al., 2000; Waizenegger et al., 2000; Adachi et al., 2008). This removal, known as the prophase pathway, allows sister chromatids to separate along their arms (but not centromeres), giving mitotically arrested chromosomes their characteristic X shape. At anaphase, the small pool of cohesin that remains at centromeres is removed by proteolytic cleavage of the kleisin subunit by the protease separase, opening the ring and enabling sister chromatids to separate. Thereafter cohesin is immediately reloaded, and the cycle continues. A variation on the cohesin cycle is observed in the budding yeast *Saccharomyces cerevisiae*, in which the prophase pathway is absent and all cohesin removal depends on separase cleavage of Scc1. Consequently new Scc1 needs to be synthesized to enable reassembly of the complex, and it is loaded later in G1 and S phase (Nasmyth and Haering, 2005, 2009; Nasmyth, 2011).

The cohesiveness of cohesin is established coincident with DNA replication and is then maintained throughout interphase by the acetylation of the Smc3 subunit (known as Psm3 in *Schizosaccharomyces pombe*) on two N-terminal lysines by homologues of human Esco1 and Esco2 (known as Eso1 in *S. pombe* and Eco1 in *S. cerevisiae*). This modification antagonizes anticonhesive functions for two cohesin regulators, Pds5 and Wapl (known as Wpl1 in *S. pombe* and Rad61 in *S. cerevisiae*; Ivanov et al., 2002; Hou and Zou, 2005; Rolef Ben-Shahar et al., 2008; Zhang et al., 2008; Rowland et al., 2009; Beckouet et al., 2010). Pds5 has complex functional relationships with Eso1: both overexpression and deletion of *pds5* suppress the lethality of *eso1Δ* and *eso1-H17* (a temperature-sensitive allele) in *S. pombe* (Tanaka et al., 2001). Further, Pds5 and Eso1 physically interact, and Pds5 promotes the acetylation of the Smc3 homologue Psm3 by Eso1, thus also promoting the cohesiveness of cohesin (Vaur et al., 2012). The nonlinear nature of these interactions makes genetic analyses of these interactions complex and needs to be interpreted in light of all available data, cell cycle position, and presence of DNA damage.

The mitotic defects conferred by Smc5/6 dysfunction in *S. pombe* are characterized by sister centromere separation at anaphase without sister chromatid arm separation. This occurs spontaneously in null mutants and in hypomorphs after DNA damage or replication stress (Verkade et al., 1999; Harvey et al., 2004). The mitotic failure is due to the postanaphase retention of cohesin on chromosome arms but not centromeres (Outwin et al., 2009; Tapia-Alveal et al., 2014a,b), that is, a failure of the prophase pathway. Although the mechanism leading to cohesin retention is not yet clear, the mitotic defects can be overcome by ectopic expression of separase (Outwin et al., 2009) and the loss of the histone variant H2A.Z (Tapia-Alveal et al., 2014b); both of these scenarios significantly lower arm cohesin levels, although H2A.Z levels have little to no effect on centromeric cohesin. A similar dependence on Smc5/6 for cohesin removal has been found in *S. cerevisiae* during meiosis (Copsey et al., 2013) but not during mitosis (Jeppsson et al., 2014), in which the prophase pathway does not function. Of note, the genomic locations of cohesin and Smc5/6 are largely overlapping (Pebernard et al., 2008; Jeppsson et al., 2014), and thus there is significant cross-talk between these related complexes (Tapia-Alveal et al., 2014a).

Coincident with the predominance of the separase pathway in *S. cerevisiae*, nonacetylatable (K-to-R) *smc3* mutants are lethal, as is the deletion of *PDS5*. The lethality of mutations in this region of Smc3 is suppressed, however, upon deletion of *ECO1* (Rowland et al., 2009). However, nonacetylatable *psm3-RR* mutants are viable in *S. pombe* (Feytout et al., 2011), and *pds5* is not an essential gene (Wang et al., 2002). On the other hand, *eso1* is an essential gene, but the lethality of *eso1⁻* mutants is still suppressed by *pds5Δ* and *wpl1Δ* (Tanaka et al., 2001; Feytout et al., 2011; Vaur et al., 2012). Thus Eso1 either has another substrate and/or another function(s) in addition to Psm3 acetylation that is essential for cell viability, and Pds5 and Wpl1 remain antagonists of these.

Here we study the essential nature of *eso1* in *S. pombe*. We show that the terminal phenotype of *eso1-H17* is mitotic arrest due to activation of the spindle assembly checkpoint. This is induced by premature separation of centromeres, although is not related to Psm3 acetylation status. Instead, this is associated with a depletion of Pds5 from centromeres. This defect is bypassed in Smc5/6 mutants, which in turn has its cohesin-retention defects suppressed by Eso1 inactivation. This extends the functional interactions of cohesin and Smc5/6 and also identifies a novel noncatalytic role for Eso1 in centromere cohesion. Given the similarity in cohesin cycles between *S. pombe* and humans, this new function for Eso1 and Smc5/6 is likely to be conserved in organisms that use the separase-independent pathway to reset the cohesin cycle.

RESULTS

Eso1 inactivation activates a lethal spindle checkpoint arrest

To understand why *eso1* is an essential gene whereas Psm3 acetylation is not required for cell viability, we first characterized the terminal phenotype of a temperature-sensitive lethal *eso1* allele, *eso1-H17*. At 25°C, *eso1-H17* grows normally and resembles wild-type cells. At restrictive temperatures (32–36°C), ~50% of *eso1-H17* cells arrest in mitosis with short bipolar mitotic spindles (Figure 1A).

We then screened for extragenic suppressors of *eso1-H17*. To avoid reisolating suppressor mutations in *pds5* and *wpl1*, we duplicated these genes in the *eso1-H17* genome, selected spontaneous suppressors by plating cells at restrictive temperature, and identified the suppressing mutation by whole-genome resequencing. Among the suppressors was a frameshift mutation in the spindle assembly checkpoint (SAC) kinase gene *bub1*, truncating the protein at residue 106 (N-terminal to the kinase domain; Figure 1B). We confirmed suppression of both growth (Figure 1C) and spindle morphology (Figure 1A) with null alleles of both *bub1* and *mad2*. Thus the lethality of *eso1-H17* is SAC dependent.

Because the spindles were normal in appearance (Figure 1A), we tested whether the SAC was being activated by premature centromere separation. To this end, we used strains with a lacO array integrated immediately adjacent to the centromere on chromosome 2, with lacI–green fluorescent protein (GFP) expressed constitutively from the *his7* promoter (Outwin et al., 2009). To distinguish premature separation from normal separation, this was done on a temperature-sensitive *cut9-665* genetic background; Cut9 is a component of the anaphase-promoting complex, and inactivation of Cut9 induces a metaphase arrest with paired centromeres (Samejima and Yanagida, 1994). This experiment showed premature separation in ~35% of *eso1-H17* cells (Figure 1D). Although lower than the percentage of cells with short spindles (~50%, Figure 1A), this is likely an underestimate of actually separated centromeres that are not far enough apart to distinguish optically. A similar experiment using a lacO array integrated at the *ade8* locus, which also on chromosome 2 but ~2.5 Mb from the centromere, was also performed. *eso1-H17*

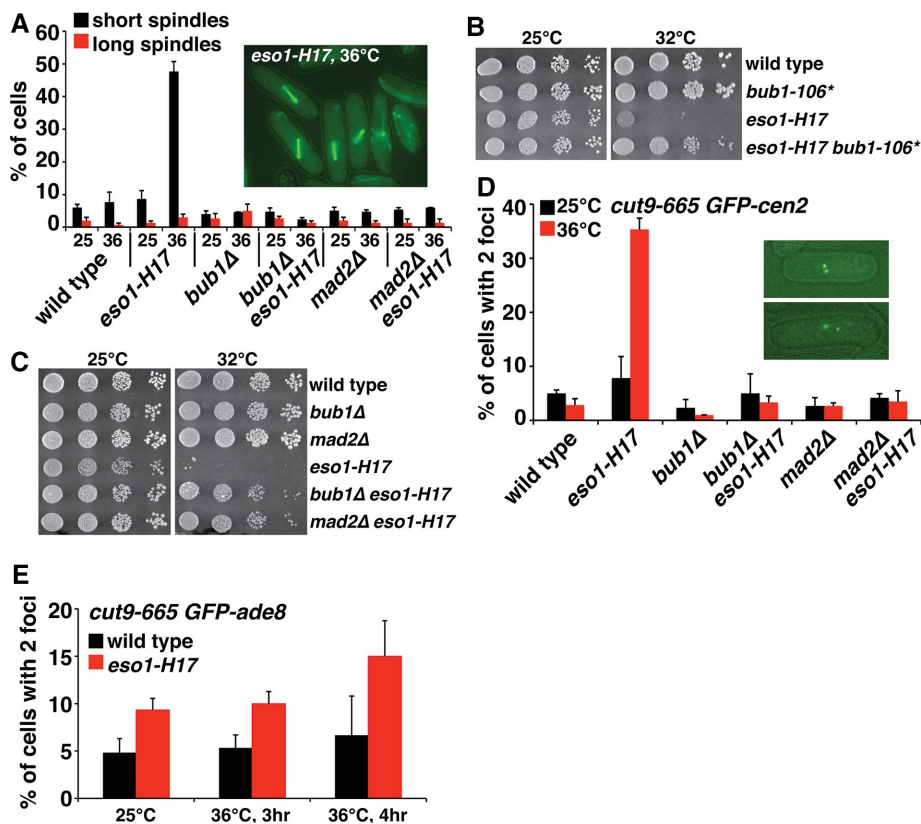


FIGURE 1: *eso1-H17* lethality is due to spindle assembly checkpoint activation by premature centromere separation. (A) The indicated strains expressing GFP-tagged α -tubulin were grown at 25°C and then shifted to 36°C for 4 h. The percentage of cells with either short (black) or long (red) spindles were quantified in three counts of 100 cells. Data are mean \pm SD. Inset, sample image of *eso1-H17* at 36°C. (B, C) An extra copy of the *pds5* and *wpl1* genes was integrated into the genome of *eso1-H17* cells, which were propagated at 32–36°C, whereupon rare ($<10^{-9}$) spontaneous suppressors arise. Suppressing mutations were identified by whole-genome resequencing of both parental and suppressor strains. A frameshift mutation in *bub1* resulting in a stop codon at codon 106 (*bub1-106**) was identified as suppressing the lethality of *eso1-H17* (B) and further confirmed with null alleles of both *bub1* and *mad2* (C). (D) The indicated strains with the temperature-sensitive APC/C mutant *cut9-665*, a LacO array adjacent to centromere 2 and expressing GFP-LacI, were grown at 25°C (black) or shifted to 36°C for 4 h to arrest cells in metaphase (red). The percentage of cells with two visibly separate GFP foci was quantified from three counts of 100 cells. Data are mean \pm SD. Inset, examples of *eso1-H17* cells with two foci. (E) Separation of the *ade8* locus, located 2.5 Mb from the *cen2* on the right arm of chromosome 2, was assayed as in D.

had an increase in separation of this locus at all temperatures, but the effect was less than half that seen for the centromeres (Figure 1E). As expected, *bub1* Δ also suppressed this premature-centromere-separation phenotype (Figure 1D). Thus inactivation of Eso1 manifests in the cohesion of centromeres, leading to SAC activation. However, whatever the SAC activating defect is, it is not by itself a lethal event.

Spindle checkpoint arrest is not due to N-terminal Psm3 hypoacetylation

The best-characterized function for Eso1 is the enforcement of cohesin's cohesiveness via acetylation of K105 and K106 on the Smc3 homologue, Psm3 (Feytout *et al.*, 2011). Using a strain with both these lysines mutated to arginines (*psm3-RR*), we assessed spindle morphology and frequency and observed no accumulation of short spindles (Figure 2A).

This suggested that SAC activation upon *Eso1-H17* inactivation should not correlate with Psm3's acetylation status. To assess this,

we used an acetyl-specific antibody for K106 (K106^{Ac}; Feytout *et al.*, 2011), and indeed, we could not detect Psm3 acetylation in *eso1-H17* cells grown at 25, 30, or 36°C (Figure 2B). The same result was also reported for *eso1-H17* grown at 25°C by Feytout *et al.* (2011), who kindly provided the K106^{Ac} antibody. In addition, we generated a second *eso1* allele, *eso1-1*. This has two point mutations, R810G and K811G. The analogous mutations in *ECO1* in *S. cerevisiae* were originally reported to lack activity in vitro when purified from bacteria (Ivanov *et al.*, 2002) but were subsequently shown to retain some autoacetyltransferase activity when purified from *S. cerevisiae* extracts (Unal *et al.*, 2008). In *S. pombe*, *eso1-1* cells have significantly reduced K106 acetylation, which is further reduced with increasing temperature to barely detectable levels at 36°C (Figure 2B). Despite this, *eso1-1* cells grow normally (see later discussion of Figure 6E) and do not display mitotic defects. Thus we conclude that the SAC activation upon *Eso1* inactivation reflects a function other than Psm3-K106 acetylation—most likely a noncatalytic function.

Eso1 inactivation reduces centromeric Pds5

Cohesin levels at the centromeres are higher than on chromosome arms (Outwin *et al.*, 2009; Tapia-Alveal *et al.*, 2014b). As a cohesin regulator, the most obvious reason for the premature separation of centromeres was the absence of cohesin at this locus. We assayed this by chromatin immunoprecipitation (ChIP) and found no effect of *eso1-H17* on cohesin at the outer repeats (OTRs) of the centromeres (Figure 3A). However, the OTRs must be separated, as the lacO arrays are adjacent to them but further away from the innermost repeats of the centromeres. Thus, although present,

the centromeric cohesin in *eso1-H17* cells cannot be cohesive at 36°C. We also observed no significant change in cohesin levels in subtelomeric DNA (STE1) or at loci on each of the chromosome arms (1L–3R), although, presumably, cohesiveness is also affected at these loci (cf. Figures 3A and 1E).

Another cohesin regulator is Pds5, with complex functional relationships with Eso1 (Tanaka *et al.*, 2001; Wang *et al.*, 2002). However, through a physical interaction between Pds5 and Eso1, Pds5 is believed to promote Psm3 acetylation and promote sister chromatid cohesion (Vaur *et al.*, 2012). We assayed the localization of Pds5 to the same loci used for the cohesin ChIP experiments (Figure 3B). Indeed, at 36°C in *eso1-H17* cells, Pds5 levels were reduced at the centromeres by ~70%. It was also reduced at some arm loci but not to the same extent as at the centromeres. Thus a defect in Eso1-dependent recruitment of Pds5 is likely at least one aspect of the centromere defect in *eso1-H17*. However, this cannot alone explain *eso1*'s essential nature, as *pds5* Δ cells are viable, albeit with mitotic defects (Tanaka *et al.*, 2001; Wang *et al.*, 2002).

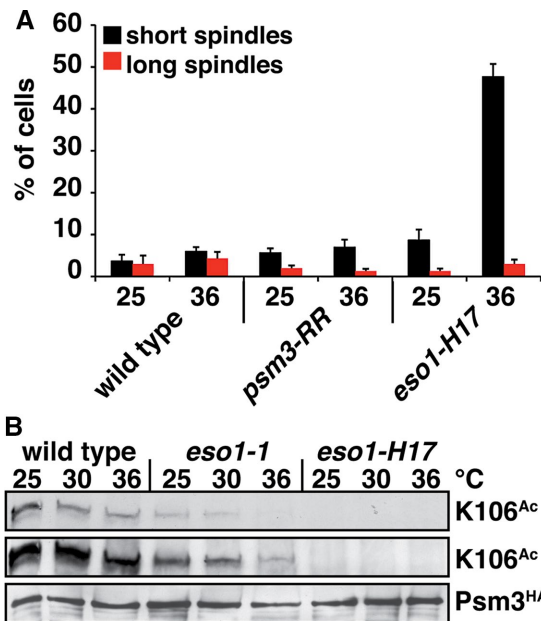


FIGURE 2: Spindle checkpoint activation is not caused by Psm3 hypoacetylation. (A) Wild-type, nonacetylatable *psm3-RR* and *eso1-H17* cells expressing GFP-tagged α -tubulin were grown at 25°C and then shifted to 36°C for 4 h. The percentage of cells with either short (black) or long (red) spindles was quantified in three counts of 100 cells. Data are mean \pm SD. (B) Western blot of total (anti-HA) and K106-acetylated (K106^{Ac}) Psm3 in the indicated strains at 25, 30, and 36°C (4 h each). The K106^{Ac} blots are a short (top) and long (middle) exposure of the same Western. This membrane was stripped and reprobed for anti-HA (bottom).

Spindle checkpoint activation in *eso1-H17* is bypassed by *Smc5/6* dysfunction

Previously we showed that the cohesin-related *Smc5/6* complex mediates cohesin dynamics in *S. pombe*. *Smc5/6* is required for the separate-independent prophase pathway of cohesin removal from chromosome arms; *Smc5/6* genes are essential, but this defect can be induced in hypomorphs such as *smc6-74* by DNA damage and replication stress (Outwin *et al.*, 2009; Tapia-Alveal *et al.*, 2014a,b). Although *Smc5/6* does not mediate centromeric cohesin removal, we believed it was possible that *Smc5/6* (as a cohesin regulator) and *Eso1* might interact in the regulation of centromeric separation. Indeed, *smc6-74* completely suppressed the SAC-activation (Figure 4A) and premature-centromere-separation (Figure 4B) phenotypes of *eso1-H17* but did not restore colony formation at nonpermissive temperatures (see later discussion of Figure 6D). Because *smc6-74* cells have no spindle defect on their own (Verkade *et al.*, 1999), there is no interaction with SAC mutants (unpublished results). Of interest, this suppression mechanism did not restore Pds5 recruitment to the centromeres (Figure 4C), and changing *pds5* gene copy number does not alter the phenotype (unpublished results). Thus either this suppression is a bypass suppression mechanism or, despite the cohesion-promoting activity of Pds5, its absence from centromeres in *eso1-H17* is not functionally significant in the premature centromere separation in *eso1-H17*.

Damage-induced cohesin retention after *Smc5/6* dysfunction does not require additional cohesin loading

To further explore the relationship between *Smc5/6* and *Eso1*, we next asked whether the damage-induced cohesin retention in irradiated *smc6-74* cells is the preexisting cohesin complexes in G2 cells

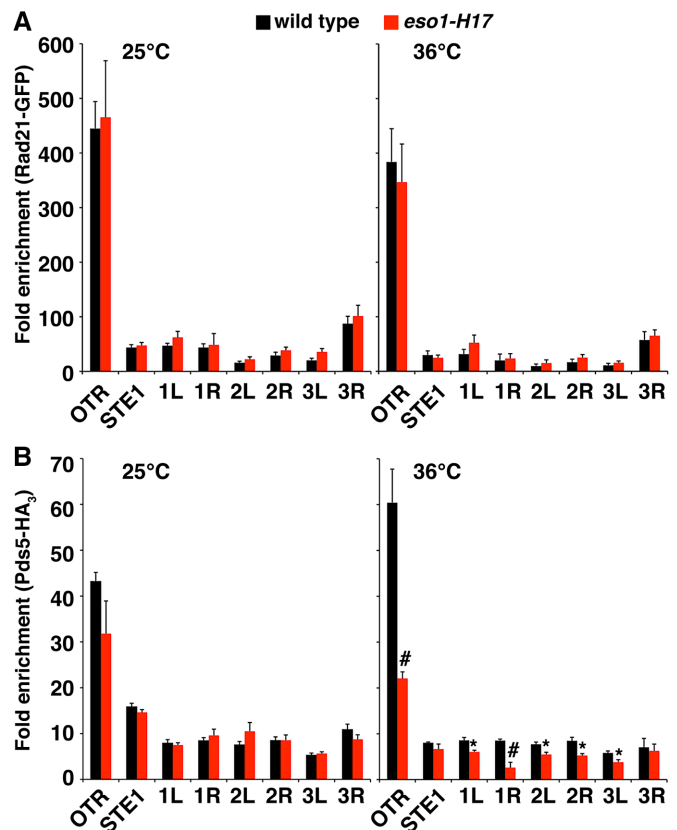


FIGURE 3: *Eso1* inactivation depletes Pds5, but not cohesin, from centromeres. (A) Cohesin (Rad21-GFP) and (B) Pds5 (Pds5-HA₃) levels were assayed by ChIP in wild-type (black) and *eso1-H17* (red) cells grown at 25°C or shifted to 36°C for 4 h. Loci are the outer repeats of the centromeres (OTR), subtelomeric DNA on chromosome 2R (STE1), and each chromosome arm (1L–3R). Data (qPCR) are mean \pm SEM, $n = 6$. Two-sided *t* test comparing wild type to *eso1-H17*: # $p < 0.001$, * $p < 0.05$. Nonannotated histogram bars represent nonsignificant differences.

already acetylated by *Eso1* or newly recruited complexes at sites of DNA damage. This was designed to ask whether the observed retention required loading of cohesin to sites of DNA damage or, alternatively, whether the regular existing complexes were the retained pool of cohesin. To this end, we devised a protocol in which *Mis4* inactivation (using temperature-sensitive *mis4-242*) blocks additional cohesin loading in cells before irradiation, and then we assayed arm and centromere separation microscopically (Figure 5, A and D). Compared to wild-type controls (Figure 5B), *smc6-74* cells showed the same chromosome arm segregation defects regardless of *Mis4* status (Figure 5C), indicating that it is the existing pool of arm cohesin that is retained in *smc6-74*.

Cosuppression of mitotic defects after *Eso1* and *Smc5/6* dysfunction

Because the presence of cohesin on chromosomes does not indicate its cohesive state (e.g., Figure 3A), we used *Mis4* inactivation in synchronized cells to study the dynamics of cohesin that is regulated by *Smc5/6*. We attempted to extend these studies to ask how *eso1* affects the dynamics regulated by *Smc5/6* after DNA damage or replication stress, but double mutants of both *eso1-H17* and *eso1-1* with *mis4-242* are close to synthetic lethal at 25°C (unpublished data) and too severely growth inhibited to make meaningful conclusions. We therefore devised a protocol using hydroxyurea (HU)

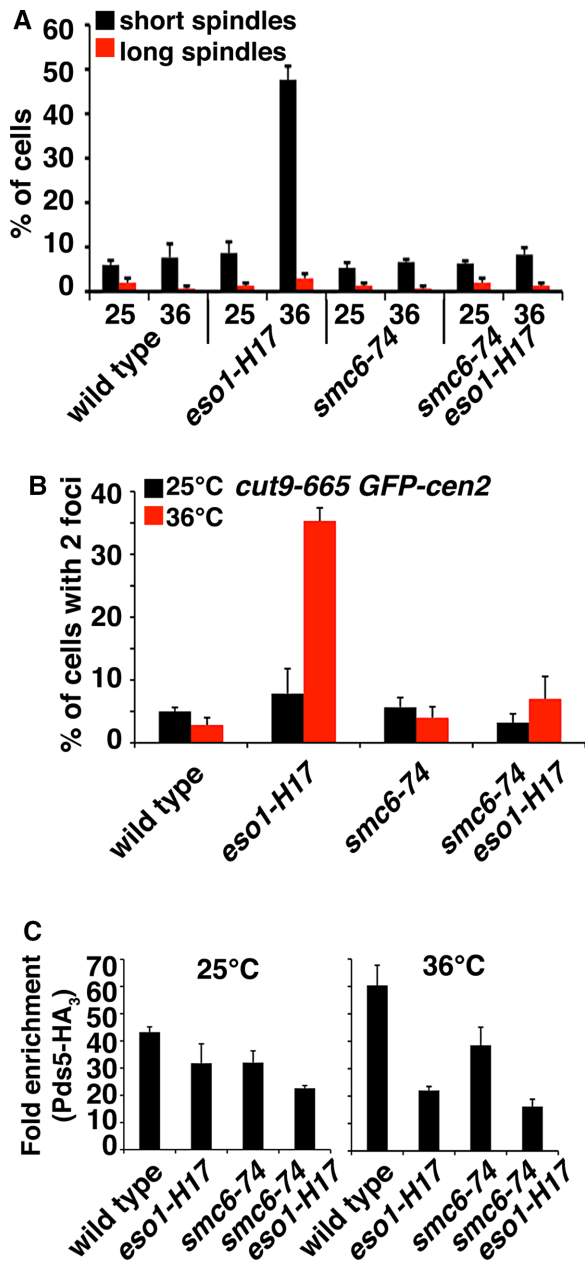


FIGURE 4: Spindle checkpoint activation in *eso1-H17* requires Smc5/6 function. (A) The indicated strains expressing GFP-tagged α -tubulin were grown at 25°C and then shifted to 36°C for 4 h. The percentage of cells with either short (black) or long (red) spindles was quantified in three counts of 100 cells. Data are mean \pm SD. Short spindle accumulation in *eso1-H17* is suppressed by *smc6-74*. (B) Premature centromere separation was assayed in the indicated strains as performed in Figure 1D. The accumulation of cells with separated centromere 2 in *eso1-H17* is suppressed by *smc6-74*. (C) The indicated strains were grown at 25°C or shifted to 36°C, and Pds5 levels at the centromeres (OTR) were determined as in Figure 3. Despite suppression, *smc6-74* does not restore depleted Pds5 levels in *eso1-H17*.

block and release, which both induces cohesin retention in *smc6-74* (Outwin *et al.*, 2009) and allows analysis of chromosome segregation and viability as cells synchronously pass through a single mitosis (Figure 6A). We combined this with temperature shifts to modulate Eso1-H17 activity. Of interest, this protocol showed *eso1-H17* to be extremely HU sensitive at all temperatures, even more so than

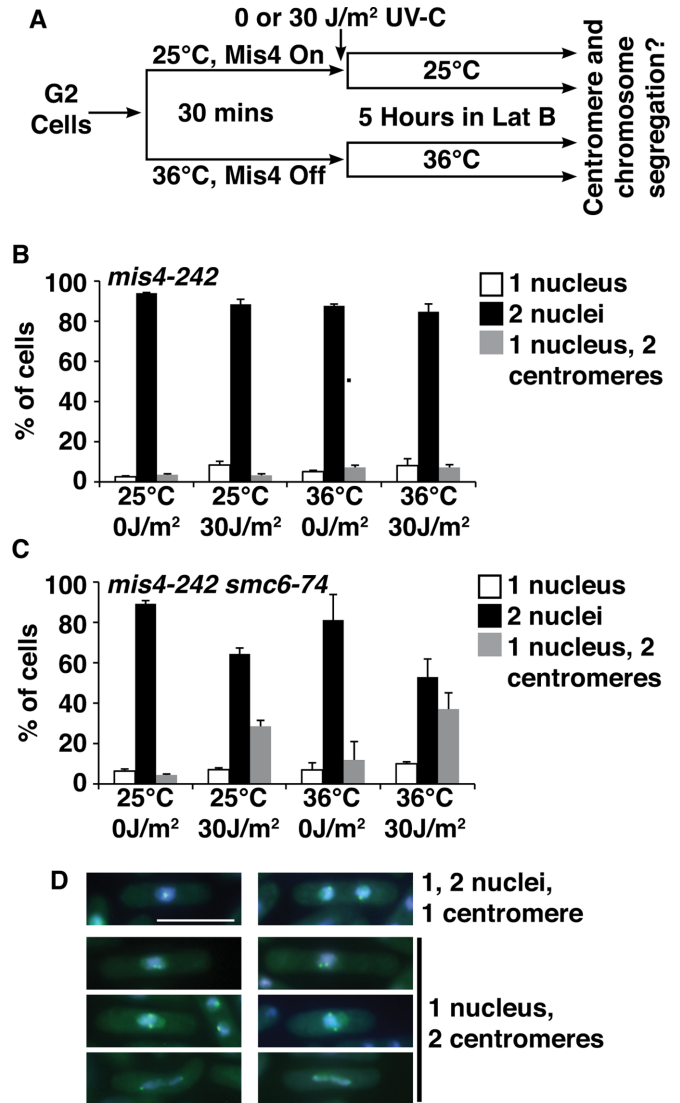


FIGURE 5: Preexisting cohesin complexes are retained following DNA damage in *smc6-74* cells. (A) The experimental protocol. *mis4-242* cells expressing a GFP-lacI fusion and carrying a lacO array directly adjacent to centromere 2 were used on both wild-type and *smc6-74* backgrounds. G2 cells were collected by elutriation at 25°C, split, and then either left to recover at 25°C for 30 min or shifted to 36°C to thermally inactivate *mis4-242* and prevent further loading of cohesin. Cells were then filtered and irradiated with 0 or 30 J/m² ultraviolet-C and returned to growth at 25 or 36°C for a further 5 h in the presence of the actin poison latrunculin B (10 μ M; to prevent lethal cytokinetic events). Cells were then scored for nuclear and GFP focus number by microscopy. (B) Data from *mis4-242* cells. (C) Data from *mis4-242 smc6-74* cells. Data are mean \pm SD for three counts of >100 cells. Note that cen2 separates without chromosome segregation (one nucleus, two centromeres) regardless of Mis4 status in *smc6-74* cells. (D) Micrographs of merged DAPI and GFP signals showing normal cells with one or two nuclei (top) and examples of the aberrant mitoses seen in irradiation *smc6-74* cells. Bar, 10 μ m.

smc6-74. However, *smc6-74 eso1-H17* double mutants showed co-suppression; that is, the double mutants completed mitosis more efficiently than the parental single mutants and had better corresponding survival (Figure 6, B and C) in this HU block-and-release protocol. This was not seen in colony formation assays on HU-containing plates at 25°C, or at 32°C without HU, but this would require

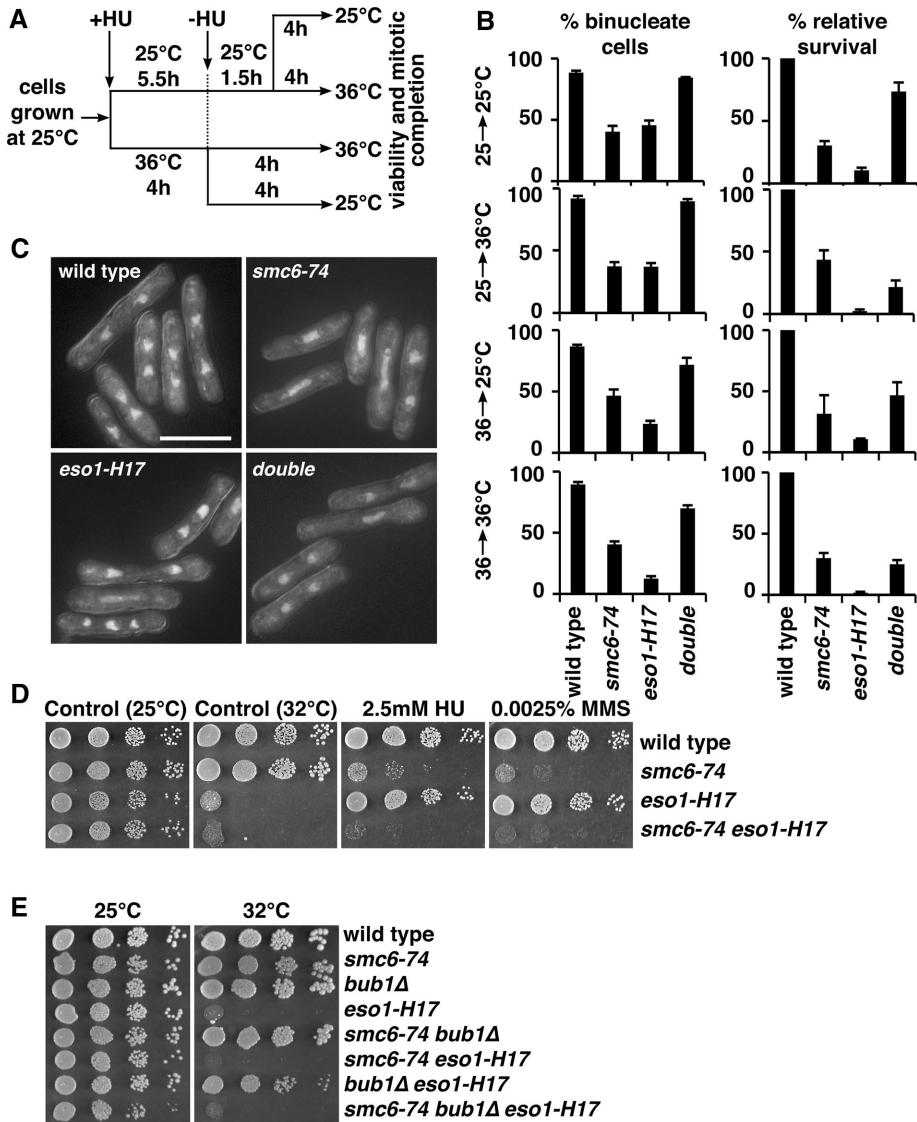


FIGURE 6: Cosuppression between *smc6-74* and *eso1-H17* restores viability and mitotic completion. (A) The experimental protocol. Cells growing asynchronously at 25°C were treated with 11 mM HU and then left at 25°C for 5.5 h or shifted to 36°C for 4 h (cell cycle equivalents). HU was then removed by filtration, and cultures were split to 25 or 36°C for 4 h ± 10 μM latrunculin B. For cultures treated at 25°C, an additional 1.5 h was added at 25°C to allow completion of DNA replication before temperature shift. (B) Aliquots were taken from the 10 μM latrunculin B cultures, fixed, and stained with DAPI to assess percentage of normal binucleated cells (data are mean ± SD of >100 cells, n = 3). Aliquots were taken from the 0 μM latrunculin B cultures, serially diluted, plated to YES plates to assess relative viability compared with no-HU controls, and normalized to wild type (mean ± SD, n = 3). Note that regardless of temperature protocol, HU induces a blockade to anaphase in *smc6-74* and *eso1-H17* cells, but this is cosuppressed in the double mutant. (C) Micrographs of DAPI-stained cells of the indicated strains after incubation at 36°C in the presence of latrunculin B. The aberrant mitoses seen in *smc6-74* and *eso1-H17* cells are characteristic of all temperature combinations. Bar, 10 μm. (D) The cosuppression does not extend to colony formation at 32°C over 4 d or in the presence of methyl methanesulfonate (MMS) or HU over 5 d at 25°C. (E) SAC inactivation (*bub1Δ*) does not confer colony formation on *smc6-74 eso1-H17* cells.

efficient suppression over ~40 cell cycles (Figure 6D). On long incubations, in liquid cultures, the double mutants accumulate cells that are dying in mitosis, and this is in keeping with the substantial but incomplete suppression. Similarly, *smc6-74 eso1-H17 bub1Δ* triple mutants also fail to form colonies at nonpermissive temperatures (Figure 6E).

Cosuppression was not seen with the *psm3-RR* mutant (Figure 7A), nor does this modify the sensitivity of *smc6-74* to chronic exposure of low-dose HU (Figure 7B). However, in keeping with the cohesin-retention defects in this strain, acetyl-mimic (cohesion-promoting) *psm3-NN* did increase the HU sensitivity of *smc6-74* (Figure 7B). Suppression by both protocols was also not seen with *eso1-1* (Figure 7C), despite significantly reduced Psm3-K106 acetylation (Figure 2B). Because Eso1 in *S. pombe* is a fusion protein in which the acetyltransferase domain is fused to the bypass polymerase Polη, we deleted that polymerase domain and confirmed no interaction with *smc6-74* (Figure 7D; Sheedy et al., 2005; Lee et al., 2007). Finally, we assayed HU sensitivity in cells lacking *bub1* or *mad2* and observed efficient suppression of the HU sensitivity of *eso1-H17*. Therefore SAC activation is the source of HU sensitivity of *eso1-H17* cells (Figure 7E).

Thus we conclude that the observed cosuppression of HU-induced mitotic failure is not due only to Psm3 hypoacetylation, although this may contribute in part to the suppression of the cohesin retention leading to HU-induced mitotic failure in *smc6-74*. In turn, the suppression of SAC activation by *smc6-74* reverses the HU sensitivity of *eso1-H17*, indicating that HU-induced replication stress potentiates the centromeric defects caused by Eso1 dysfunction.

DISCUSSION

Many aspects of the regulation of the cohesin cycle have been firmly established in several experimental systems. Most notable among these is the budding yeast *S. cerevisiae*. In this system, cohesin's cohesiveness appears to be largely regulated by Eco1-catalyzed Smc3 acetylation and the subsequent blocking of antiohesive factors, and this activity is required for cell viability. In turn, removal of cohesin at anaphase in this organism seems also to be via one molecular event: the cleavage of Scc1 by separase (Nasmyth and Haering, 2009).

Although these events are conserved across eukaryotes, they appear to control only a subset of cohesin complexes. At least in *S. pombe*, Psm3 acetylation is dispensable for cell viability (Feytout et al., 2011). Similarly, in human cells, induced expression of nonacetylatable Smc3 has relatively modest effects on sister chromatid cohesion (Zhang et al., 2008), although this is in the presence of wild-type Smc3. However, at least in human cells, Smc3 acetylation does promote the processivity of DNA replication fork processivity (Terret et al., 2009) and, coupled with the role of cohesin as a transcriptional insulator (Wendt et al., 2008), provides possible alternative explanations for phenotypes associated with Smc3 hypoacetylation.

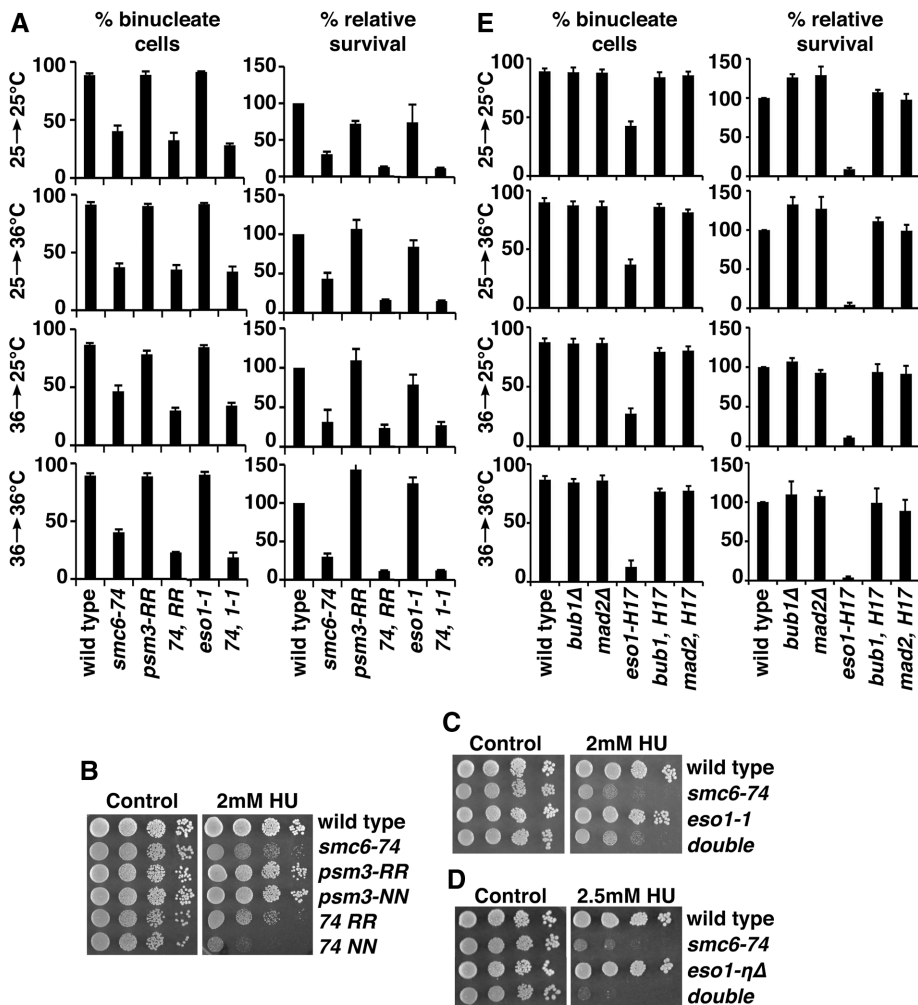


FIGURE 7: Blocking Psm3 acetylation does not phenocopy *eso1-H17*. (A) The same protocol used in Figure 6 was used to assess suppression of *smc6-74* by the nonacetylatable *psm3-RR* mutant and the acetyl-low *eso1-1* mutant. In no case was suppression observed. Unlike *eso1-H17*, *eso1-1* shows neither HU-induced mitotic defects nor suppression of *smc6-74* despite a significant reduction in Psm3 K106 acetylation (Figure 2). (B) Acetyl-mimetic (*psm3-NN*) enhances the HU and MMS sensitivity of *smc6-74*, but nonacetylatable (*psm3-RR*) does not. (C) *eso1-1* does not suppress the chronic HU sensitivity *smc6-74*. (D) A strain in which the DNA polymerase η domain region of *eso1* is deleted (*eso1- $\eta\Delta$*) does not suppress the HU or MMS sensitivity of *smc6-74*. (E) The same HU block-and-release protocol used in Figure 6A was used to assess the effects of SAC mutations on the HU sensitivity of *eso1-H17*, which was suppressed by both *bub1 Δ* and *mad2 Δ* .

Despite the viability of *psm3-RR* mutants, *eso1* is an essential gene in *S. pombe*. Because SAC ablation suppresses the lethality of *eso1-H17* (Figure 1), an important component of the essential function(s) of Eso1 resides in promoting the cohesion of sister centromeres in a manner independent of acetylation of Psm3, at least on K105 and K106. Although it is possible that Eso1-H17 retains acetyltransferase activity for other sites and/or other proteins, no other acetylation sites in cohesin can be detected with anti-acetyl-lysine antibodies (Feytout *et al.*, 2011). We tagged *eso1* and *eso1-H17* with various epitopes, and whereas Eso1-H17 protein is expressed at all temperatures, epitope-tagged *eso1-H17* is only viable on a *pds5 Δ* background at 25°C (unpublished data), and so addition of the tags renders the protein completely nonfunctional. Nevertheless, it suggests that the temperature sensitivity of *eso1-H17* is not associated with degradation of the protein.

Note that suppression of the growth defect of *eso1-H17* by *mad2 Δ* was previously observed (Tanaka *et al.*, 2000), but evidence of SAC activation and premature centromere separation was not reported. Our results show that cohesin is present at centromeres in *eso1-H17* (Figure 3A), but as centromeres prematurely separate, these cohesin complexes cannot be cohesive. What is depleted from the centromeres in *eso1-H17* is Pds5 (Figure 3B), and because the interaction between Pds5 and Eso1 promotes cohesiveness (Vaur *et al.*, 2012), this defect is a likely cause of the premature centromere separation. Analyzing *pds5 Δ* cells cannot mimic this because they will also be defective in cohesion regulation on the arms.

We also observed strong functional interactions between *smc6-74* and *eso1-H17*. The blockade to sister chromatid separation caused by the retention of existing arm cohesin complexes in *smc6-74* cells after DNA damage or replication stress is also suppressed by *eso1-H17* (Figures 5 and 6). Of note, centromeric cohesin and cohesion are unaffected in *smc6-74* and other Smc5/6 mutants (Outwin *et al.*, 2009; Tapia-Alveal *et al.*, 2014a,b). Because acetyl-mimetic *psm3-NN* enhances the HU sensitivity of *smc6-74* (Figure 7B), the suppressing effects of *eso1-H17* are likely to be, at least in part, via Psm3 hypoacetylation. This was not seen with *psm3-RR*, which may not recapitulate the spatial control of Psm3 acetylation and/or may indicate an additional level of regulation that relieves cohesin retention in the face of Smc5/6 dysfunction. Chemical (thiabendazole) or genetic (*nda3-KM311* at 18°C) activation of the SAC by tubulin depolymerization does not suppress *smc6-74* (unpublished data), suggesting that this is not the source of *smc6-74* suppression.

In turn, the suppression of the premature centromere separation of *eso1-H17* must be either independent of Pds5 recruitment or a compensatory bypass of this defect. Lethal SAC activation is potentiated in *eso1-H17* by replication stress, which may exacerbate defective DNA replication in the absence of Eso1 function. Of note, the resident heterochromatin and repetitive nature of the centromeres make these difficult-to-replicate regions of the genome (Hayashi *et al.*, 2009; Li *et al.*, 2013). Whatever the molecular centromeric defect in *eso1-H17*, the suppression by *smc6-74* suggests that it includes the Smc5/6-dependent formation of toxic structures that are further promoted by extrinsic replication stress. With its well-defined role in controlling recombination at both stably stalled and collapsed replication forks (Ampatzidou *et al.*, 2006; Murray and Carr, 2008; Irmisch *et al.*, 2009), the combination of *smc6-74* with *eso1-H17* may prevent such structures from forming. Testing and refining such a hypothesis will first require a better understanding of the centromeric function for Eso1. Although this is a problem that will require substantial future work, it is at least an area of

investigation that begins to bring together what we know about cohesin, Smc5/6, and their regulators.

In cells in which a genetically or chemically induced molecular defect activates a cell cycle checkpoint, the viability of such cells is usually dependent on an intact checkpoint response. This is not the case for *eso1-H17*, for which SAC activation is actually the lethal response. Thus the centromeric defect conferred by *Eso1* dysfunction is tolerable, albeit checkpoint activating.

Many aspects of the cohesin cycle are conserved between *S. pombe* and humans. Thus it will be important to understand whether there is a centromeric function for human ESCO1/2, as well as the relationship between the spindle checkpoint and ESCO1/2 (and other cohesin and Smc5/6 components) in the developmental disorders and cancers in which these genes are mutated (Skibbens *et al.*, 2013; Price *et al.*, 2014; Cucco and Musio, 2016; van der Crabben *et al.*, 2016). Indeed, SAC dysfunction may be an explanation as to why some tumor cells can survive loss-of-function mutations in cohesin, whereas normal cells cannot.

MATERIALS AND METHODS

S. pombe culture and genetic methods

All strains were constructed by tetrad analysis, with compound mutants selected from non-parental ditypes. In each case, multiple progeny were analyzed and backcrossed to exclude the presence of suppressor mutations. Cells were grown in supplemented yeast extract plus glucose (YES) or EMM2 (Moreno *et al.*, 1991). Culture methods for individual experiments are described in the relevant figure legends. Drug sensitivity assays were performed on solid YES medium, with 5- μ l drops of 10-fold serial dilutions from cultures containing $\sim 4 \times 10^6$ cells/ml and plates photographed after either 4 d (30°C) or 5 d (25°C). Ultraviolet-C sensitivity was determined by triplicate plating of 100–10,000 cells, which, after drying, were irradiated in a Stratalinker (Stratagene, San Diego, CA). Viability assays were determined by triplicate plating of a culture dilution series to YES and normalized to untreated wild-type cells. *eso1-1* was constructed by fusion PCR and integration into the *eso1* locus and confirmed by sequencing and Southern blotting. G2-synchronized cells were obtained by centrifugal elutriation using a Beckman (Brea, CA) JE-5.0 elutriation system. Strains are listed in the Supplementary Material.

Screen for suppressors of *eso1-H17*

eso1-H17 cells were transformed with genomic clones of both *pds5* and *wpl1*. Single-copy integrants (at *leu1* and *nmt1*, respectively) were selected and confirmed to phenocopy untransformed *eso1-H17* cells. Spontaneous suppressors were selected and identified by whole-genome resequencing as previously described (Tapia-Alveal *et al.*, 2014b).

Microscopy

Nuclei were visualized in cells fixed in 70% ethanol by staining with 1 μ g/ml 4',6-diamidino-2'-phenylindole dihydrochloride (DAPI). Microtubules were visualized in live cells expressing GFP-tubulin. Spindles were scored as short when present as newly growing spindles through to those as long as the diameter of an undivided nucleus (~ 0.5 – 3.5μ m). On anaphase, short spindles rapidly elongate to a length of $\sim 10 \mu$ m, which were scored as long spindles. Intermediates are rarely observed but were scored as long when nuclear division was advancing. Centromere 2 was visualized in either live cells immobilized on thin agarose pads by expression of GFP-LacI from the *his7* promoter in strains with a lacO array integrated immediately adjacent to the outer repeat (OTR; Outwin *et al.*, 2009) or cells fixed in 90% methanol, stained with DAPI, and imaged immediately. Arm

separation was assayed with a lacO array at the *ade8* locus (Outwin *et al.*, 2009). Microscopy was carried out on a Zeiss (Thornwood, NY) Z1 Imager with a 100 \times /1.4 Pan-Apo objective.

Protein extracts and Western blotting

To detect total and acetylated Psm3, cells were grown to mid logarithmic phase at 25°C and shifted to either 30 or 36°C for 4 h. Cells were harvested by centrifugation and snap frozen in liquid nitrogen. Cells were then disrupted in a mini beadbeater (Biospec) using the following buffer: 50 mM 4-(2-hydroxyethyl)-1-piperazineethanesulfonic acid, pH 7.5, 100 mM KCl, 2.5 mM MgCl₂, 0.25% Triton X-100, 1 mM dithiothreitol, 0.1% SDS, 10 mM sodium butyrate, 10% glycerol, 1 mM sodium orthovanadate, 20 mM β -glycerophosphate, 1 mM phenylmethylsulfonyl fluoride, and 5 \times protease inhibitor cocktail (P8340; Sigma-Aldrich, St. Louis, MO). Protein levels were quantified (Dc Protein assay; Bio-Rad), and 30 μ g was separated on a 6% SDS-PAGE gel. Proteins were transferred to nitrocellulose in 10 mM 3-(cyclohexylamino)-1-propanesulfonic acid and 10% methanol at 70 V and 45 min. The membrane was blocked in Tris-buffered saline containing 0.1% Tween 20 (TBST) and 5% skim milk powder for 30 min. K106-acetylated Psm3 was detected with a 1:2000 dilution of an acetyl-specific antibody overnight (Feytout *et al.*, 2011), followed by a 1:2000 dilution of horseradish peroxidase HRP-conjugated anti-rabbit immunoglobulin G (IgG; GE Healthcare). Immune complexes were detected with Clarity Reagent (Bio-Rad). Subsequently the membrane was stripped with 200 mM sodium hydroxide for 2 \times 10 min at room temperature, rinsed in TBST, and reprobed with 0.04 μ g/ml anti-hemagglutinin (HA; 12CA5; Roche) overnight, followed by 1:2000 HRP-conjugated anti-mouse IgG and detected with Clarity Reagent.

Chromatin immunoprecipitation

Methods for ChIP and primer sequences for quantitative PCR (qPCR) were as previously described (Outwin *et al.*, 2009). qPCR data are expressed as fold enrichment over an untagged isogenic control. In each case, the input DNA is 1/80 of the IPed DNA, so percentage recovery can be calculated by dividing the fold enrichment by 80. Oligonucleotides for qPCR are listed in the Supplementary Material.

ACKNOWLEDGMENTS

We thank Jean-Paul Javerzat for providing strains and the anti-K106 acetyl-Psm3 antibody and gratefully acknowledge Emily Outwin for the construction of *eso1-1*. This work was supported by National Institute of General Medical Sciences/National Institutes of Health Grant R01-GM088162 and National Cancer Institute/National Institutes of Health Grant T32-CA078207.

REFERENCES

- Adachi Y, Kokubu A, Ebe M, Nagao K, Yanagida M (2008). Cut1/separase-dependent roles of multiple phosphorylation of fission yeast cohesion subunit Rad21 in post-replicative damage repair and mitosis. *Cell Cycle* 7, 765–776.
- Ampatzidou E, Irmisch A, O'Connell MJ, Murray JM (2006). Smc5/6 is required for repair at collapsed replication forks. *Mol Cell Biol* 26, 9387–9401.
- Beckouet F, Hu B, Roig MB, Sutani T, Komata M, Uluocak P, Katis VL, Shirahige K, Nasmyth K (2010). An Smc3 acetylation cycle is essential for establishment of sister chromatid cohesion. *Mol Cell* 39, 689–699.
- Copsey A, Tang S, Jordan PW, Blitzblau HG, Newcombe S, Chan AC, Newnham L, Li Z, Gray S, Herbert AD, *et al.* (2013). Smc5/6 coordinates formation and resolution of joint molecules with chromosome morphology to ensure meiotic divisions. *PLoS Genet* 9, e1004071.

- Cucco F, Musio A (2016). Genome stability: what we have learned from cohesinopathies. *Am J Med Genet C Semin Med Genet* 172, 171–178.
- Feytout A, Vaur S, Genier S, Vazquez S, Javerzat JP (2011). Psm3 acetylation on conserved lysine residues is dispensable for viability in fission yeast but contributes to Eso1-mediated sister chromatid cohesion by antagonizing Wpl1. *Mol Cell Biol* 31, 1771–1786.
- Harvey SH, Krien MJ, O'Connell MJ (2002). Structural maintenance of chromosomes (SMC) proteins, a family of conserved ATPases. *Genome Biol* 3, REVIEWS3003.
- Harvey SH, Sheedy DM, Cuddihy AR, O'Connell MJ (2004). Coordination of DNA damage responses via the Smc5/Smc6 complex. *Mol Cell Biol* 24, 662–674.
- Hayashi MT, Takahashi TS, Nakagawa T, Nakayama J, Masukata H (2009). The heterochromatin protein Swi6/HP1 activates replication origins at the pericentromeric region and silent mating-type locus. *Nat Cell Biol* 11, 357–362.
- Hirano T (2005). Condensins: organizing and segregating the genome. *Curr Biol* 15, R265–R275.
- Hirano T (2006). At the heart of the chromosome: SMC proteins in action. *Nat Rev Mol Cell Biol* 7, 311–322.
- Hou F, Zou H (2005). Two human orthologues of Eco1/Ctf7 acetyltransferases are both required for proper sister-chromatid cohesion. *Mol Biol Cell* 16, 3908–3918.
- Irmisch A, Ampatzidou E, Mizuno K, O'Connell MJ, Murray JM (2009). Smc5/6 maintains stalled replication forks in a recombination-competent conformation. *EMBO J* 28, 144–155.
- Ivanov D, Schleiffer A, Eisenhaber F, Mechtler K, Haering CH, Nasmyth K (2002). Eco1 is a novel acetyltransferase that can acetylate proteins involved in cohesion. *Curr Biol* 12, 323–328.
- Jeppsson K, Carlborg KK, Nakato R, Berta DG, Lilienthal I, Kanno T, Lindqvist A, Brink MC, Dantuma NP, Katou Y, et al. (2014). The chromosomal association of the Smc5/6 complex depends on cohesion and predicts the level of sister chromatid entanglement. *PLoS Genet* 10, e1004680.
- Lee KM, Nizza S, Hayes T, Bass KL, Irmisch A, Murray JM, O'Connell MJ (2007). Brc1-mediated rescue of Smc5/6 deficiency: requirement for multiple nucleases and a novel Rad18 function. *Genetics* 175, 1585–1595.
- Li PC, Petrea RC, Jensen A, Yuan JP, Green MD, Forsburg SL (2013). Replication fork stability is essential for the maintenance of centromere integrity in the absence of heterochromatin. *Cell Rep* 3, 638–645.
- Merkenschlager M, Odom DT (2013). CTCF and cohesin: linking gene regulatory elements with their targets. *Cell* 152, 1285–1297.
- Moreno S, Klar A, Nurse P (1991). Molecular genetic analysis of fission yeast *Schizosaccharomyces pombe*. *Methods Enzymol* 194, 795–723.
- Murray JM, Carr AM (2008). Smc5/6: a link between DNA repair and unidirectional replication? *Nat Rev Mol Cell Biol* 9, 177–182.
- Nasmyth K (2011). Cohesin: a catenase with separate entry and exit gates? *Nat Cell Biol* 13, 1170–1177.
- Nasmyth K, Haering CH (2005). The structure and function of SMC and kleisin complexes. *Annu Rev Biochem* 74, 595–648.
- Nasmyth K, Haering CH (2009). Cohesin: its roles and mechanisms. *Annu Rev Genet* 43, 525–558.
- Outwin EA, Irmisch A, Murray JM, O'Connell MJ (2009). Smc5-Smc6-dependent removal of cohesin from mitotic chromosomes. *Mol Cell Biol* 29, 4363–4375.
- Parelho V, Hadjur S, Spivakov M, Leleu M, Sauer S, Gregson HC, Jarmuz A, Canzonetta C, Webster Z, Nesterova T, et al. (2008). Cohesins functionally associate with CTCF on mammalian chromosome arms. *Cell* 132, 422–433.
- Pebernard S, Schaffer L, Campbell D, Head SR, Boddy MN (2008). Localization of Smc5/6 to centromeres and telomeres requires heterochromatin and SUMO, respectively. *EMBO J* 27, 3011–3023.
- Price JC, Pollock LM, Rudd ML, Fogoros SK, Mohamed H, Hanigan CL, Le Gallo M, Program NI, Zhang S, Cruz P, et al. (2014). Sequencing of candidate chromosome instability genes in endometrial cancers reveals somatic mutations in ESCO1, CHTF18, and MRE11A. *PLoS One* 8, e63313.
- Rolef Ben-Shahar T, Heeger S, Lehane C, East P, Flynn H, Skehel M, Uhlmann F (2008). Eco1-dependent cohesin acetylation during establishment of sister chromatid cohesion. *Science* 321, 563–566.
- Rowland BD, Roig MB, Nishino T, Kurze A, Uluocak P, Mishra A, Beckouet F, Underwood P, Metson J, Imre R, et al. (2009). Building sister chromatid cohesion: smc3 acetylation counteracts an antiestablishment activity. *Mol Cell* 33, 763–774.
- Rubio ED, Reiss DJ, Welsh PL, Distèche CM, Filippova GN, Baliga NS, Aebersold R, Ranish JA, Krumm A (2008). CTCF physically links cohesin to chromatin. *Proc Natl Acad Sci USA* 105, 8309–8314.
- Samejima I, Yanagida M (1994). Bypassing anaphase by fission yeast cut9 mutation: requirement of cut9+ to initiate anaphase. *J Cell Biol* 127, 1655–1670.
- Sheedy DM, Dimitrova D, Rankin JK, Bass KL, Lee KM, Tapia-Alveal C, Harvey SH, Murray JM, O'Connell MJ (2005). Brc1-mediated DNA repair and damage tolerance. *Genetics* 171, 457–468.
- Sjogren C, Nasmyth K (2001). Sister chromatid cohesion is required for postreplicative double-strand break repair in *Saccharomyces cerevisiae*. *Curr Biol* 11, 991–995.
- Skibbens RV, Colquhoun JM, Green MJ, Molnar CA, Sin DN, Sullivan BJ, Tanzosh EE (2013). Cohesinopathies of a feather flock together. *PLoS Genet* 9, e1004036.
- Tanaka K, Hao Z, Kai M, Okayama H (2001). Establishment and maintenance of sister chromatid cohesion in fission yeast by a unique mechanism. *EMBO J* 20, 5779–5790.
- Tanaka K, Yonekawa T, Kawasaki Y, Kai M, Furuya K, Iwasaki M, Murakami H, Yanagida M, Okayama H (2000). Fission yeast Eso1p is required for establishing sister chromatid cohesion during S phase. *Mol Cell Biol* 20, 3459–3469.
- Tapia-Alveal C, Lin S-J, O'Connell MJ (2014a). Functional interplay between cohesin and Smc5/6 complexes. *Chromosoma* 123, 437–445.
- Tapia-Alveal C, Lin SJ, Yeoh A, Jabado OJ, O'Connell MJ (2014b). H2A.Z-dependent regulation of cohesin dynamics on chromosome arms. *Mol Cell Biol* 34, 2092–2104.
- Terret ME, Sherwood R, Rahman S, Qin J, Jallepalli PV (2009). Cohesin acetylation speeds the replication fork. *Nature* 462, 231–234.
- Tomonaga T, Nagao K, Kawasaki Y, Furuya K, Murakami A, Morishita J, Yuasa T, Sutani T, Kearsey SE, Uhlmann F, et al. (2000). Characterization of fission yeast cohesin: essential anaphase proteolysis of Rad21 phosphorylated in the S phase. *Genes Dev* 14, 2757–2770.
- Unal E, Heidinger-Pauli JM, Kim W, Guacci V, Onn I, Gygi SP, Koshland DE (2008). A molecular determinant for the establishment of sister chromatid cohesion. *Science* 321, 566–569.
- van der Crabben SN, Hennus MP, McGregor GA, Ritter DI, Nagamani SC, Wells OS, Harakalova M, Chinn IK, Alt A, Vondrova L, et al. (2016). Destabilized SMC5/6 complex leads to chromosome breakage syndrome with severe lung disease. *J Clin Invest* 126, 2881–2892.
- Vaur S, Feytout A, Vazquez S, Javerzat JP (2012). Pds5 promotes cohesin acetylation and stable cohesin-chromosome interaction. *EMBO Rep* 13, 645–652.
- Verkade HM, Bugg SJ, Lindsay HD, Carr AM, O'Connell MJ (1999). Rad18 is required for DNA repair and checkpoint responses in fission yeast. *Mol Biol Cell* 10, 2905–2918.
- Waizenegger IC, Hauf S, Meinke A, Peters JM (2000). Two distinct pathways remove mammalian cohesin from chromosome arms in prophase and from centromeres in anaphase. *Cell* 103, 399–410.
- Wang SW, Read RL, Norbury CJ (2002). Fission yeast Pds5 is required for accurate chromosome segregation and for survival after DNA damage or metaphase arrest. *J Cell Sci* 115, 587–598.
- Wendt KS, Yoshida K, Itoh T, Bando M, Koch B, Schirghuber E, Tsutsumi S, Nagae G, Ishihara K, Mishiro T, et al. (2008). Cohesin mediates transcriptional insulation by CCCTC-binding factor. *Nature* 451, 796–801.
- Zhang J, Shi X, Li Y, Kim BJ, Jia J, Huang Z, Yang T, Fu X, Jung SY, Wang Y, et al. (2008). Acetylation of Smc3 by Eco1 is required for S phase sister chromatid cohesion in both human and yeast. *Mol Cell* 31, 143–151.